Genome-based Study on the Mechanism of Rare Earth Neodymium Ions Increasing Ethanol Production from *Clostridium thermocellum*

Jinna Cui,[a,b,c,d] Tiantian Sun,[a,b,c,d] Lixia Liu,[a,b,c,d] Zhanying Liu [a,b,c,d,*]

The escalating global demand for energy, coupled with heightened environmental concerns, has rendered the identification of sustainable and environmentally friendly alternative energy sources imperative. Ethanol derived from cellulosic fibers is garnering significant interest as a clean and renewable energy source. Among the various production methods, consolidated bioprocessing (CBP) stands out due to its distinct advantages. *Clostridium thermocellum* is considered an exemplary candidate strain for the CBP production of cellulosic ethanol; however, the low yield of ethanol remains a critical limiting factor. In the preceding study, it was demonstrated that neodymium ions could enhance the ethanol production of *C. thermocellum*. In this study, the whole genome sequences of the original strain *C. thermocellum* ATCC 27405 (C0) and the strain with added neodymium ions (Nd^{3+}) (C1) were sequenced and analyzed. The findings indicated that the increased expression of pyruvate-ferric redox protease (PFO) resulted from mutations in its promoter region. Furthermore, an analysis of the sequencing data, along with the results from single knockout experiments, revealed that mutations in the genes encoding methyl-accepting chemotaxis proteins (MCP) and type 3a cellulose-binding domain protein (Type) genes were correlated with enhanced ethanol production. This study serves as a reference for the targeted modification of *C. thermocellum* to optimize ethanol production.

DOI: 10.15376/biores.20.2.3155-3175

Keywords: Rare earth; Neodymium ions; Clostridium thermocellum; Ethanol; Genome; Gene knockout

Contact information: a: Center for Energy Conservation and Emission Reduction in Fermentation Industry in Inner Mongolia, Inner Mongolia University of Technology, Hohhot, 010051, Inner Mongolia, China; b: Engineering Research Center of Inner Mongolia for Green Manufacturing in Bio-fermentation Industry, Inner Mongolia University of Technology, Hohhot, 010051, Inner Mongolia, China; c: Specialized Technology Research and Pilot Public Service Platform for Biological Fermentation in Inner Mongolia, Hohhot, 010051, Inner Mongolia, China; d: College of Chemical Engineering, Inner Mongolia University of Technology, Hohhot, 010051, Inner Mongolia, China;
** Corresponding author: hgxylzy2008@imut. edu.cn*

INTRODUCTION

Since the industrial revolution, fossil fuels such as coal and oil have become essential for human production and life (Hosseini *et al*. 2013). While the widespread use of these energy sources has greatly boosted productivity, it has also resulted in significant greenhouse gas emissions, contributing to global warming (Jayakumar *et al*. 2023). In response to these challenges, many countries are now exploring biomass resources to create biofuels, which offer a renewable energy alternative that can greatly reduce greenhouse gas emissions and support environmentally sustainable development (Qiao *et al*. 2022;

Nawab *et al*. 2024). According to the report by the International Energy Agency (IEA), biofuels are currently a commercially produced alternative fuel compared to other alternative fuels, with the potential to replace 10% of global oil, based on fuel performance, infrastructure, and other factors. Biofuel represents a viable alternative fuel that fulfills the criteria of being renewable, environmentally friendly, and capable of large-scale production.

Cellulosic ethanol, as a typical biofuel, is fermented and converted from fibrous materials such as straw, hulls, skins and stalks of crops, residues from wood processing, and organic wastes from cities and villages (Myat *et al*. 2015; Guo *et al*. 2022). Cellulosic ethanol has many advantages, such as non-pollution, short regeneration period, and no increase in the total amount of greenhouse gases (Lovett *et al*. 2011). The utilization of lignocellulosic feedstock for ethanol production can mitigate the reliance on food sources for ethanol, thereby reducing competition for food resources among populations. This approach not only has beneficial implications for environmental sustainability, but it also contributes positively to the overall sustainable development of society (Reijnders *et al*. 2007). For example, Yu *et al*. (2014) obtained a theoretical ethanol yield of 69.5% under optimal conditions using sweet sorghum bagasse as fermentation substrate. Zheng *et al*. (2021) produced cellulosic ethanol from sugarcane bagasse (SCB) with an ethanol yield of 257 ± 5.51 mg/g SCB, which was produced at low cost and with high energy efficiency.

The *Thermoanaerobacterales,* which exhibit a notable capacity for ethanol production, encompass genera such as *Geobacinus*, *Thermoanaerobacter*, and *Clostridium*. For instance, research have used *Thermoanaerobacterium aotearoense* (Fu e*t al.* 2019) or *Thermoanaerobacterium saccharolyticum* (Desai *et al.* 2004) for fermentation to produce ethanol and improved yields through genetic engineering techniques. *Clostridium thermocellum* (*C. thermocellum*) is one of the few microorganisms that can directly use cellulose fermentation to produce ethanol in the natural environment as the second generation biofuel with its unique advantages as a sustainable energy source (Chang *et al.* 2013; Qiao *et al*. 2022). The *C. thermocellum*, a thermophilic, strictly anaerobic gram-positive bacterium, is one of the most efficient cellulose-degrading bacteria available. It metabolizes natural products including ethanol, acetic acid, lactic acid, formic acid, and hydrogen (Mazzoli *et al.* 2014; Liu *et al*. 2020; Xiao *et al*. 2023). *C. thermocellum* is able to produce decomposable cellulosic material (fibrous vesicles) due to its own properties, which contain a variety of hydrolytic enzymes, glycosidases, lichen polysaccharidases, hemicellulases, and so on (Bayer *et al*. 2004; Levin *et al*. 2006; Zhang *et al*. 2017; Jiang *et al*. 2021). However, the low yield and low feedstock utilization of *C. thermocellum* for cellulosic ethanol has limited its further industrial application. Currently, pretreatment processes have the capacity to alter the intricate structure of cellulose, thereby enhancing the efficiency of raw material utilization. Various pretreatment techniques have been identified, including mechanical grinding (Zeng *et al.* 2010), ultrasonics (Liyakathali *et al.* 2016), and acid or alkaline hydrolysis (Sindhu *et al.* 2014; Nur Aimi *et al.* 2015). Fermentation using treated feedstocks can improve utilization and yield. To further improve ethanol production, researchers have conducted studies related to the conversion of lignocellulose to ethanol by *C. thermocellum* in terms of metabolic pathways, cellulose degradation mechanisms, and ethanol fermentation. Biswas *et al*. (2015) obtained a mutant strain of *C. thermocellum* that was functionally deficient in all hydrogenases by gene knockout, resulting in 64% of the maximum theoretical yield of ethanol. Kannuchamy *et al*. (2016) transformed pyruvate decarboxylate (PDC) and alcohol dehydrogenase (ADH)

genes from *Zymomonas mobilis* into *C. thermocellum*, which resulted in a twofold increased pyruvate decarboxylase activity and ethanol production.

In the 1970s, researchers identified that rare earth ions exert an activating effect on cellulases, amylases, and proteases (Darnall and Birnbaum 1970; Gomez *et al*. 1974; Diatloff *et al*. 1995; Zhang *et al*. 2009). When the catalytic activity of the same enzyme is in the presence of various rare earth ions, complex reaction phenomena occur due to differences in the composition and structure of the enzyme's active center, the active center and its surroundings, and the mode of substrate action. This indicates that the relationship between rare earth ions and enzyme activity is highly complex, necessitating further comprehensive investigations to elucidate the underlying mechanisms. Inspired by the idea of rare earth ions to increase enzyme activity, Xin *et al*. (1996) demonstrated that several low concentrations of rare earth ions increased the activity of glutamate dehydrogenase. Since 2012, the authors' research laboratory has been focused on improving bioethanol production through rare earth ions. Although significant advancements have been made in this area, the existing literature on the application of rare earth ions to enhance ethanol production *via* microbial fermentation remains limited. Genome sequencing represents a critical step in the correlation of genotypes with phenotypic characteristics. This process entails the submission of the genome sequence of an unidentified species to a gene sequencer, detecting the signal of its bases, and then stitching it together (Joan *et al*. 2019; Singh *et al*. 2022). In particular, the technical means of triple sequencing, developed on the basis of the original sequencing technology, can obtain higher quality genome sequences and provide technical support for in-depth studies of bacteria. Yayo *et al*. (2021) identified two potential mutation sites by genome sequencing, gene editing, and physiological characterization of *C. thermocellum* and found that these mutations play a role in the transport or metabolism of hexoses.

In previous stages of this experiment, *C. thermocellum* ATCC27405 and *T. thermosaccharolyticum* DSM571 were used to produce fuel ethanol by co-fermentation. The processes were regulated from multiple perspectives, including inoculation time, inoculation ratio, substrate concentration, fermentation temperature, pH, and metal ions, so as to optimize the ethanol yield (Pang *et al*. 2018a,b). Wang *et al.* treated *C. thermocellum* ATCC27405 (C0) with 10^{-6} mol/L Nd^{3+}, and the highest ethanol yield of the strain was 1.05 g/L with 26.6% ethanol yield, which was 97.5% higher than C0 (Wang *et al.* 2022). However, the specific mechanism of action of neodymium ions at the genomic level is not clear. The enzyme expression is regulated by various factors such as promoter sequences, enhancer sequences, and RNA polymerase activity, with the promoter being the most critical and direct factor. If the key site of the promoter can be found, then the yield can be further improved by genetic engineering. Based on previous studies, this study mainly analyzed the mechanism of Nd^{3+} to increase ethanol production of *C. thermocellum* C0 from the promoter sequence and genome level of key enzymes that include alcohol dehydrogenase (ADH), pyruvate-ferric redox protease (PFO), and 6-phosphofructokinase (PFK). Through studying the mechanism of Nd^{3+} on the metabolic pathway of *C. thermocellum*, the targeted transformation of the strain and the analysis of the metabolic pathway, this study serves as a reference for future research aimed at enhancing ethanol yield.

EXPERIMENTAL

Strains and Culture Media

The original strain utilized in this study was *C. thermocellum* ATCC27405, subsequently designated as *C. thermocellum* C0. The strain *C. thermocellum* C1 underwent treated with Nd^{3+}, and it was conserved in the Chinese Center for Typical Cultures Collection (CCTCC) under the conservation number CCTCC NO: M2021190. The strain exhibiting point mutations in the promoter sequences of the three key enzymes has been designated as *C. thermocellum* C3.

The medium was prepared in an anaerobic cabinet with an atmosphere of N_2, and the medium composition and configuration methods were according to Wang *et al.* (2022). The 5% (v/v) inoculum was inoculated in 100-mL serum bottles and incubated at 55 °C and 180 r/min for 12 h.

Methods

The Nd^{3+} treatment method

The medium was supplemented with 10^{-6} mol/L of Nd^{3+} and incubated continuously for six generations. Then, 5% (v/v) of *C. thermocellum* C0 strain containing Nd^{3+} was inoculated into solid medium and incubated at 55 °C with stirring at 180 r/min for three days. Large colonies were inoculated into liquid medium and cultured until the logarithmic phase, which was the removal of Nd^{3+} from the medium.

Amplification and sequencing of target genes

The promoter sequences of key enzymes were sequenced by constructing recombinant plasmids. The pMD19-T Vertor (see Fig. 1) was used for the experiment, and double digestion was performed using the enzymatic sites on the primers (see Table 1).

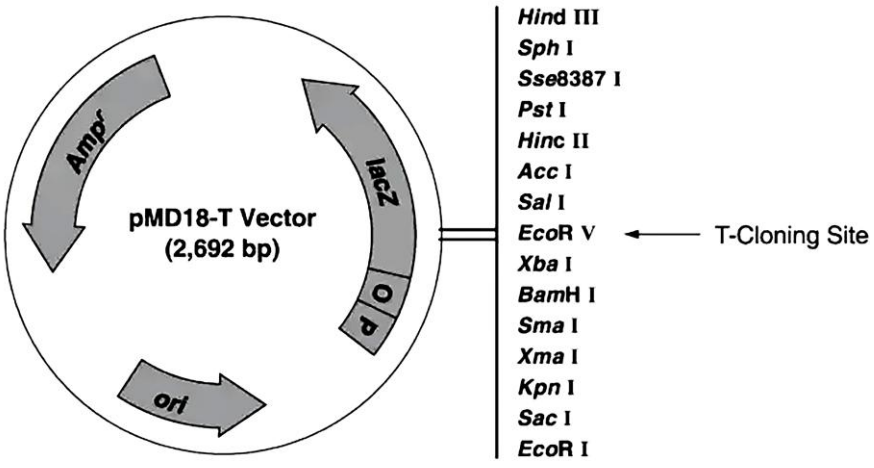

Fig. 1. pMD19-T Vertor cloning site

First, when the C0 and C1 were cultured to logarithmic phase, the DNA was extracted using the TIANGEN bacterial whole genome DNA extraction kit. The DNA of strains C0 and C1 were used as templates to amplify promoter gene fragments. The promoter gene fragments of the two strains were amplified separately, and the reaction systems included 10 μL Exq mix dye, 1 μL DNA template, 0.5 μL upstream primer, 0.5

μL downstream primer, and 8 μL ddH2O. The polymerase chain reaction (PCR) reaction system was as follows: 95 °C for 120 s, followed by 30 cycles of 95 °C for 30 s, 45 to 55 °C for 30 s, and 72 °C with the time determined by the size of the target fragment. Next, the target fragments were recovered using the Agarose Gel Recovery Kit (Tengen Biochemical Technology (Beijing) Co.). Then, the target fragment was ligated onto the pMD19-T Vertor, and the ligation system was placed in the PCR instrument at 16 °C overnight. The ligation system was 4 μL target fragment, 1 μL pMD19-T Vertor, and 5 μL Solution I. Finally, *Hind* III and *Bam*H I were used for digestion, and the recombinant plasmid with correct digestion verification was sent to Sangon Biotech (Shanghai) Co., Ltd. for sequencing.

Table 1. The Primer Sequences

Target Sequence	Primer
ADH	Upstream primer: CGAAGCTTGTTGTCAATCAAATCGCG
	Downstream primer: CGCCGGATCCTAAAACCTCCTCCTTT
PFK	Upstream primer: CGGCGAAGCTTATAATAAGCGTCAGAATGC
	Downstream primer: AATTGGATCCCTCCCCTAAATCCCGT
PFO	Upstream primer: GCAAGCTTGATTTGCAGCCGGAGTT
	Downstream primer: CGGGATCCCTCTCCTATTCTTTCCCGTT
ADH1	Upstream primer: GCATGGTAAGGAGAATAAGCATTGTACATATCGGAG
	Downstream primer: GGCAGCGTACCATTCCTCTTATTCGTAACAT
ADH2	Upstream primer: GCGCCGTGGATACTACCTCTACAAAGAACGATAT
	Downstream primer: CCGTGGCAAAAACCTATGGATGGAGATT
ADH3	Upstream primer: CTTGCGAGAGAATGCAATATGGTGACG
	Downstream primer: CCGCACCTACCTTATTAACGCTCTTCTTACG
PFO1	Upstream primer: GCCGCAGAAAATAAATGAGTATACTCCGGATGT
	Downstream primer: CGCGCCGCCACTAAAATATGTCTTTTATTTACTCT
PFO2	Upstream primer: CCGACTCCGGATGTTATTGATGAAAATCAGAAAG
	Downstream primer: CGCCGCACTCATATGAGGCCTACAATAACTT
PFO3	Upstream primer: GGCCCAGGATAAATTGATTGCAGAGTGCTTTTAC
	Downstream primer: CGCCGCCTATAAACAGGATAAATTGATTGA
PFO4	Upstream primer: CGAGTATTGGATGCAGATTTTATTTCCGACGAAG
	Downstream primer: GCCGCAATAAACCCTTTTCATAACCTACGTCTAC
PFK1	Upstream primer: AAGCTCGGCTATATTGAAAAAACGCACATTTC
	Downstream primer: TACCGCCTAAACCTCTTCGAGCCGATAT
PFK2	Upstream primer: GCGCAAATTTTATCCGACCTGACGAACT
	Downstream primer: GCTTTTCAGCCGCGTTTAAAATAGGCTG
PFK3	Upstream primer: CAAATCGTTCCGCACAACGAACAGACA
	Downstream primer: CAACTTTTGGCCCAGCACTAGGCGTGT

Note: The underlined portion represents the enzyme cleavage site, and the *Bam*H I enzyme cleavage site is GGATCCD, the *Hind* III enzyme cleavage site is AAGCTT.

Validation of promoter site-directed mutagenesis

The C0 genome was used as the template to amplify the ADH, PFK, and PFO promoter mutation sequences, respectively. The PCR amplification products were sequentially subjected to gel electrophoresis, and the gel recovery purified products were ligated with pMD19-T Vertor to construct recombinant plasmids, which were named pMD19-ADH, pMD19- PFK, and pMD19-PFO, respectively. Multiple rounds of PCR were performed for point mutation and transformation into *E. coli* DH5α receptor cells to screen positive clones with ampicillin. Ultimately, the recombinant plasmids were

extracted in limited quantities, and the positive recombinant plasmids were identified through double digestion before being sent to Sangon Biotech (Shanghai) Co., Ltd. for sequencing.

The expression vector for the experiment was pET-28a (as in Fig. 2). The pMD19-T is a cloning vector, which is mainly used for gene cloning and amplification, while pET-28a is an expression vector, which is used to express the exogenous genes in the host cells. The pMD is the high copy plasmid, which would replicate a lot of plasmids, and then enzymatically cleave to propose the target fragment inside, which would be relatively easy to be attached to the PET. After extracting the plasmids, double digestion was performed using the enzymatic sites on the primers (see Table 1), respectively. Enzymatic digestion was performed at 37 °C for 4 h. The results were examined by 1% agarose gel electrophoresis after the reaction was completed. The mutant promoter and the large fragment sequence of the expression vector were recovered, and the vector sequence was ligated to the mutant promoter. The reaction system consists of 9 μL Insert fragment, 2 μL T4 DNA Ligase Buffer, 1 μL T4 DNA Ligase, 5 μL ddH_2O, and 3 μL Vector pET-28a.

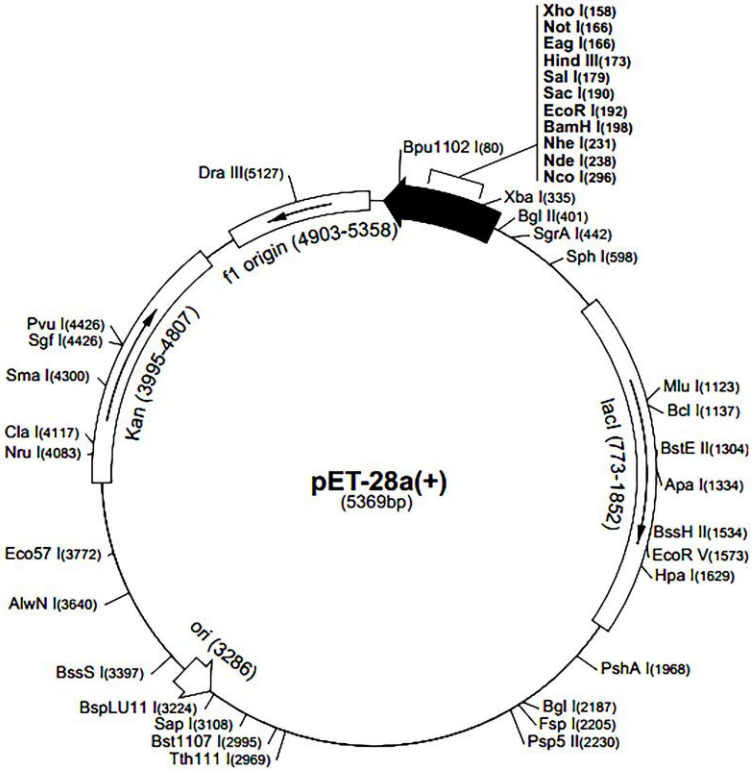

Fig. 2. pET-28a Vector map

Determining the expression of key enzymes

The bacterial broth of C0 and mutant strain (C3) were taken under the same culture conditions, and the same bacterial concentration of both strains was ensured by protein content assay. The total RNA of each strain was extracted separately using the BBI Bacterial Total RNA Rapid Extraction Kit (Sangon Biotech (Shanghai) Co., Ltd., Order NO.B518625). Then, the first strand of cDNA was synthesized using the BBI cDNA First Strand Synthesis Kit (Sangon Biotech (Shanghai) Co., Ltd., Order NO.B639251). The cDNAs of C0 and C3 were used as templates for PCR reaction amplification. The reaction

system consists of 10 μL Exq mix Dyes, 2 μL DNA template, 0.5 μL upstream primer, 0.5 μL downstream primer, and 7 μL ddH_2O. The PCR reaction system was as follows: 94 °C for 120 s, followed by 30 cycles of 94 °C for 30 s, 59 °C for 30 s, and 72 °C for 600 s. The 16S rRNA was selected as the internal reference gene. The four pairs of primers are shown in Table 2.

Table 2. Primer Design

Target Sequence	Sequence Length (bp)	Primer
16S rRNA	93	Upstream primer: CGGGTGTTGCAGACTCTCAGGTGT Downstream primer: AGTAVGGCCGCAAGGTTGAAACTCA
ADH	152	Upstream primer: CGGGTGTTGCAGACTCTCAGGTGT Downstream primer: AGTAVGGCCGCAAGGTTGAAACTCA
PFK	252	Upstream primer: GGAGCAAGAGACATCAGCAAACT Downstream primer: CAGAACGACAGCCTCAGCACCT
PFO	165	Upstream primer: GGACAACAAAGATGAGGCTGAA Downstream primer: GCCCATCCGTCTCCACCTA

The cDNA synthesized by reverse transcription of RNA from C0 and C3 was used as template and amplified by RT-PCR reaction using a fluorescent quantitative PCR instrument (BIO-RAD, Hercules, CA, USA), and the PCR reaction system was the same as above. The reaction system consisted of 10 μL Light Cycler 480 mix Dyes, 5 μL cDNA template, 1 μL upstream primer, 1 μL downstream primer, and 3 μL Light Cycler 480 DEPC H_2O. The standard curve was plotted according to the logarithm of the copy number of the standards and the Ct value. The 16S rRNA genes were used as internal reference genes to analyze the relative expression of ADH, PFO, and PFK gene mRNA in C0 and C3 according to the $2^{-\Delta\Delta Ct}$ method.

Determination of key enzyme activity

The supernatant was removed through the centrifugation of 25 mL of log-phase bacterial suspension, followed by multiple rinses of the bacterial pellet with a 0.1 mol/L Tris-HCl buffer solution (pH 7.6). Subsequently, 1.5 times the volume of the precipitate was added, and the cells were lysed under ice bath conditions. The mixture was then centrifuged for 30 minutes, yielding the intracellular crude enzyme solution as the resulting supernatant. The enzyme activity of intracellular crude enzyme solution was determined by the reaction system in Table 3.

Table 3. Enzyme Reaction System

Enzymes	Reaction System
ADH	0.1 mol/L Tris-HCl (pH 7.6) buffer, 0.01 mol/L DTT buffer, 0.5 mmol/L NAD(P)H, 0.055 mol/L acetaldehyde, Crude enzyme solution
PFO	0.1 mol/L Tris-HCl (pH 7.6) buffer, 0.1 mmol/L CoA, 0.020 mol/L DTT buffer, 2 mmol/L methylviologen, 5 mmol/L Pyruvic acid, Crude enzyme solution
PFK	0.1 mol/L Tris-HCl (pH 7.6) buffer, 0.01 mol/L DTT buffer, 2 mmol/L ATP, 5 mmol/L $MgSO_4$, 0.3 mmol/L NADH, 0.05 mol/L KCl, 2 U aldolase, 2 U Phosphoglyceraldehyde isomerase,10 U Glycerol phosphate, Crude enzyme solution

The enzymatic activity of ADH was determined by reference to the method of Brown *et al*. (2011). The enzymatic activity of PFO was determined by reference to the method of Shaw *et al*. (2008). The enzymatic activity of PFK was determined by reference to the method of Sridhar *et al*. (2000).

Comparative genomic analysis

C0 and C1 strains were cultured to logarithmic phase, then 1 mL of bacterial broth was taken, and the whole genomic DNA of both strains was extracted using the Bacterial Whole Genome DNA Extraction Kit, and sequenced by Beijing Novogene Technology Co. The single nucleotide polymorphism (SNP), insertion and deletion (InDels), and Structural variation (SV) analyses were performed on the sequencing results. Based on the positional relationships and interactions between SNPs and genes, gene prediction and annotation analyses were performed using databases, such as Rapid Annotation using Subsystem Technology (RAST), Kyoto Encyclopedia of Genes and Genomes (KEGG), and the Protein Sequence Database (SwissProt) for gene prediction and annotation analysis to resolve genome-level changes in the strains before and after mutagenesis.

Knocking out key enzyme genes

C. thermocellum C0 genomic DNA was used as the template to amplify the upstream A fragment and downstream B fragment of the target gene, respectively. The reaction system consisted of 10 μL Exq mix Dyes, 2 μL DNA template, 0.5 μL upstream primer, 0.5 μL downstream primer, and 7 μL ddH_2O. The PCR reaction system was as follows: 94 °C for 120 s, followed by 30 cycles of 94 °C for 30 s, 59 °C for 30 s, and 72 °C for 600 s. Primer sequences are shown in Table 4. The amplification products were identified correctly by agarose gel electrophoresis. The gel recovery kit was used for purification and the recovered product was stored at -20 °C.

Table 4. Arac, MCP, and Type A/B Homology Arm Primer Design

Enzyme	Sequence Length	Primer
Arac-A	800 bp	Upstream primer: CGGAATTCTCCGAACAGCAGCTTGATTG Downstream primer: CCGCGCGTTAATAGTCTTTTTTCTTTACCGGAAT
Arac-B	821 bp	Upstream primer: CGCGGATGGATTCTCTAAGCAGAATGAAT Downstream primer: CAAGCTTCAAACGACCTCCTTTCATTATCG
MCP-A	800 bp	Upstream primer: CCGAATTCGCAGCAGTATGGAGTAT Downstream primer: GCCAAGGAAGGTTTGGTAGCCGTCTTGTC
MCP-B	779 bp	Upstream primer: CATGCGAGAGAACAGGCGGCATCCAAACC Downstream primer: CGAAGCTTTGTTCCAGCCTCCCTAATAC
Type-A	768 bp	Upstream primer: GCCGAATTCCTTAGCAAAAGCTCCGG Downstream primer: CCTACCGCCGTCACCTTCAATTCCTTCCC
Type-B	701 bp	Upstream primer: CGCTGTCAACGGGGAAGGAATTGAAGGTGAC Downstream primer: CGCAAGCTTCGGACCTTACGCCGTCATT

Note: The underlined portion represents the enzyme cleavage site, and the BamH I enzyme cleavage site is GGATCCD, the Hind III enzyme cleavage site is AAGCTT.

The upstream and downstream sequences of the target gene were fused and ligated by PCR. The purified upstream and downstream homologous arm fragments were mixed in a molar ratio of 1:1, and the mixed DNA fragments were used as templates for fusion

PCR with primers AF and BR. The ligated recombinant fragments were obtained, and the PCR products were purified.

Plasmid pK18mobSacB and the target fragment were digested with *Hind* III and *EcoR* I. The digestion system were 5 μL plasmid, 0.5 μL *EcoR* I, 0.5 μL *Hind* III, 0.2 μL Buffer, 2 μL MC10 × Buffer, and 11.8 μL ddH_2O. The digestion was performed at 37 °C for 4 h. The cloning site of plasmid pK18mobSacB is shown in Fig. 3. The electro transformation protocol referred to was Huang *et al*. (2015) for the electro transformation conditions of the shuttle plasmid pLuKELd *Thermoanaerobacterium aotearoense* SCUT27. The mutant was activated and the plasmid DNA was extracted as described above. A total of 1 μL of template DNA, 0.8 μL of upstream and downstream primers, 10 μL of Taq enzyme, and 7.4 μL of ddH_2O were added for PCR amplification.

The original strain (C0) and modified strains were inoculated into the culture medium respectively, and fermented at 180rpm and 55℃ for 48h. The ethanol yield was determined at the end of fermentation and C0 was used as a control.

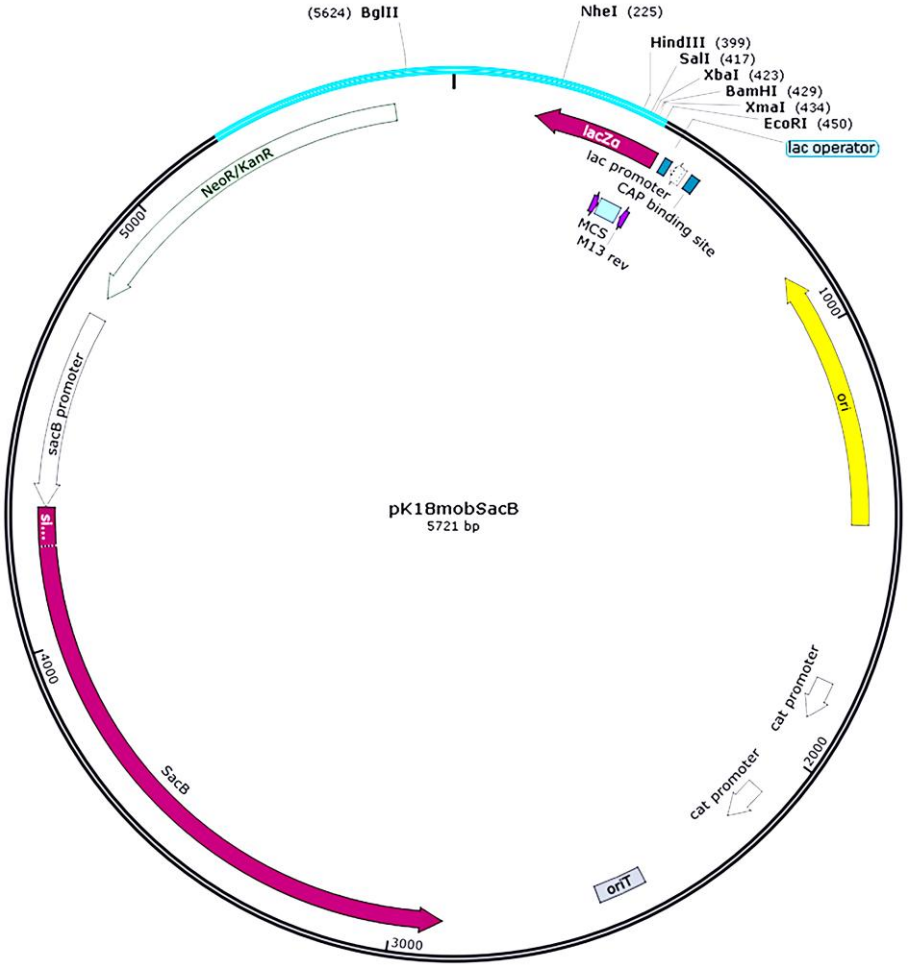

Fig. 3. Suicide plasmid pK18mobSacB map

Determination of growth curve

The wild and mutant strains were inoculated in MTC medium and incubated at 55 °C and 180 r/min for 12 h. The medium was added at 5% inoculum. The OD_{600} values were determined every 2 h and the growth curve was used to represent the growth of the strains.

Determination of ethanol yield

The ethanol content in the fermentation broth was determined by high performance liquid chromatography (e2695; Waters, MA, USA), and the liquid phase detection conditions are shown in Table 5.

Table 5. Ethanol Content Liquid Chromatography Detection Conditions

Chromatographic column type	Aminex HPX-87H column (300 mm × 7.8 mm id, 9 μm)
Mobile phase	2.5 mM H_2SO_4
Detector	Waters 2414 RI Differential detector
Flow Rate	0.5 mL/min
Sampling volume	10 μL
Column temperature	50 °C

Data analysis

The experimental data were analyzed using SAS 9.2 (SAS Inc., Cary, NC, USA) for variance analysis under $p < 0.05$ and $p < 0.01$. All data are presented as the mean ± standard deviation, ensuring a clear representation of the variability and central tendency of the observed values.

RESULTS AND DISCUSSION

Results of Promoter Sequencing Data Analysis

The strain C1 was C0 treated with the addition of Nd^{3+}. The differential gene sequences are shown in Table 6. By comparing the gene sequences of ADH, PFO, and PFK gene promoter region sequences of strains C0 and C1, three base mutations were found in the sequence of the ADH promoter region of C1 and the types of mutations were substitutions and deletions. The PFO promoter region sequence had four base substitution mutations, and the PFK promoter region sequence had three mutated bases. The bases in which substitutions and deletions occurred contained four bases, and almost all of them were mutated in a single base, indicating that neodymium ions affected the promoter region sequences of ADH, PFO, and PFK.

The initiation of transcription is a critical stage of gene expression, and when the promoter binds to RNA polymerase to start transcription, changes in the promoter structure directly affect the efficiency of binding to RNA polymerase and thus the level of gene expression (Leacock *et al*. 2006). The analysis of Nd^{3+} treatment to increase the expression level and enzyme activity of key enzyme genes may be due to the enhancement of the transcriptional function of genes by affecting the sequence of the key enzyme promoter region (Würleitner *et al*. 2003).

Table 6. Differences in Promoter Sequences of Different Genes

Gene	Base Site	C0	C1	Mutation Type
ADH	24	A	T	Reversal
	536	C	T	Reversal
	621	A	-	Deletion
PFO	76	T	A	Reversal
	96	T	C	Transition
	185	C	A	Transition
	614	T	C	Transition
PFK	16	A	G	Transition
	211	C	G	Reversal
	288	A	T	Reversal

Effect of Point Mutations of Promoter Sequence on Enzyme Expression

The key enzyme ADH, PFO, and PFK promoter region point mutant strain C3 was successfully constructed. The experimental results indicated that mutations in the promoter region of key enzymes can have an effect on the expression of key enzymes. The level of ADH gene in C3 was 1.03 times than that of C0 ($P < 0.05$), the expression of PFO gene in C3 was 1.22 times than that of C0 ($P < 0.05$), and the expression of PFK gene in C3 was 1.08 times than that of C0 ($P < 0.05$) (Fig. 4).

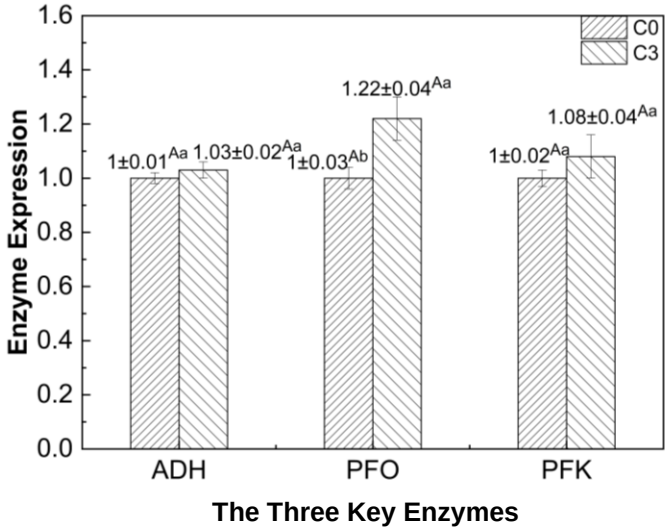

Fig. 4. The expression level of three key genes; Different lowercase letters p <0.05, and different uppercase letters p <0.01

Effect of Promoter Sequence Point Mutations on Enzyme Activity

The enzyme activities of the three key enzymes of C0 and C3 are shown in Fig. 5. The enzyme activities of ADH, PFO, and PFK in C3 were all increased compared to these in C0, being 1.05 times, 1.14 times, and 1.07 times higher than C0, respectively, but the changes of enzyme activity in these were not significant. The strength of the enzyme activity affected the efficiency of the catalysis, so the absence of significant changes in enzyme activity indicated that the catalytic capacity of the enzyme protein remained unchanged and had not affected substrate consumption and product synthesis (Petsch *et al*. 2012). The activity of enzymes depends not only on the expression level of their genes, but

also on their own structure and function. Therefore, the point mutations in promoter sequences do not necessarily cause changes in enzyme activity. The high expression of mRNA did not indicate high enzyme activity. Protein expression is closely related to transcription and translation, and its expression is determined by the transcription level and translation process (Mikel *et al*. 2021).

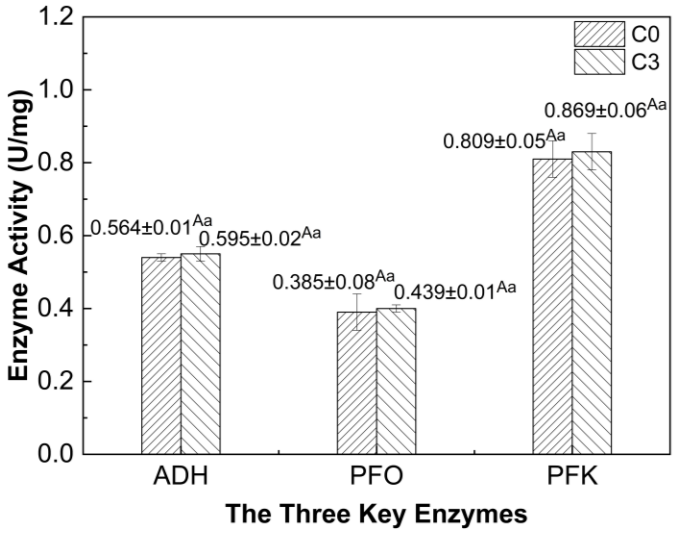

Fig. 5. Three kinds of key enzyme activity of C0 and C3; Different lowercase letters $p < 0.05$, and different uppercase letters $p < 0.01$

Key enzyme activity and expression both directly affect enzyme catalytic performance and increase the flux increase in metabolic pathways (Carere *et al*. 2014; Wang *et al*. 2022). The enzyme expression and enzyme activity are regulated by transcriptional level and gene level, *etc*. The previous study showed that Nd^{3+} can significantly increase the expression of acetaldehyde dehydrogenase (ALDH), which was 11.1 times more than the original strain. However, Nd^{3+} neither changed the gene sequences of ALDH and ADH, and nor mutated the promoter gene sequence of ALDH transcription initiation. The enzyme expression of PFK and PFO in C1 was 3.35 times and 1.53 times higher than that in C0 and the enzyme activity of PFK and PFO in CX was 2.0 times and 1.48 times higher than that of the original strain, respectively, and the gene sequences of these two enzymes were altered by Nd^{3+} (Wang *et al*. 2022). In this experiment, ADH, PFO, and PFK promoter sequences were mutated, and the fixed point mutation verified that the expression of PFO was significantly increased, which was 1.22-fold of the original strain. While the expression of ADH and PFK and the enzyme activity of the three key enzymes were not significantly changed. This indicates that the effects of mutagenesis on the structure, function, and stability of key enzyme sequences and promoters in the metabolic pathway are somewhat contingent and random and involve the regulation of other regulatory factors (Furukawa *et al*. 2009). Therefore, sequence changes in key enzyme sequences and promoter regions are not the only reason for affecting the expression and enzyme activity of key enzymes.

Results of Comparative Genomic Analysis

Through sequencing the DNA libraries of C1 and C0, the original strain sequencing data were 1358 and 1458 Mb, respectively, with a read length of 150 bp. Table 7 shows good sequencing quality. The four lines of the results of high quality library construction and sequencing were good by being close and parallel, and the GC and AT contents match well as seen in Fig. 6(a) and (b). As shown by the base quality distribution in Fig. 6 (c) and (d), the average error rate of the bases was all below 0.05%. The results indicate that the genome resequencing data have good results and can be analyzed in the next step.

Table 7. Sequencing Data Statistics

Sample ID	Insert Size (bp)	Reads Length (bp)	Raw Data (Mb)	Filtered Reads (%)	Clean Data (Mb)	GC (%)	Q20 (%)	Q30 (%)
C1	350	(150:150)	1,358	7.92	1,250	38.23	95.91	89.76
C0	350	(150:150)	1,458	7.72	1,346	38.45	95.61	89.19

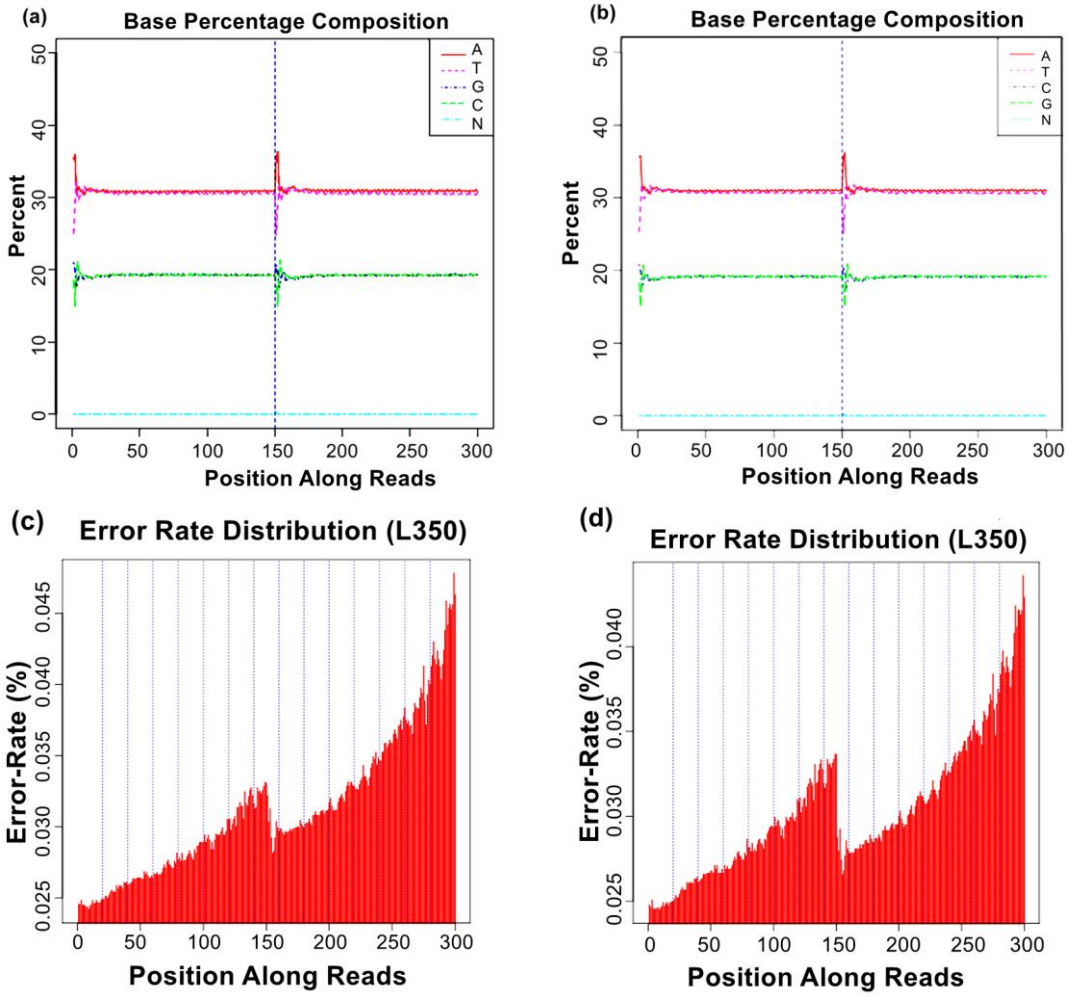

Fig. 6. Base content and base mass distribution of C0, C1: (a) C0 base mass distribution map; (b) C1 base mass distribution map; (c) C0 base mass distribution map; (d) is C1 base mass distribution map

There were 3839 and 3862 base conversions, 1261 and 1267 base reversals, 341 and 386 heterozygous SNPs, and 4759 and 4743 pure SNPs in C0 and C1, respectively. C0 has 1639 non-synonymous mutations and 2449 synonymous mutations. C1 has 1659 non-synonymous mutations and 2473 synonymous mutations. Amino acid mutations caused by nonsynonymous mutations can further affect gene expression. There were 93 mutations involving a total of 35 proteins or enzymes with mutated gene sequences. The annotation analysis yielded mutations in genes related to the biosynthesis of cell walls and cell membranes, methylotropic receptor protein genes, ribonucleases, endonuclease genes, transcriptional regulators, methyltransferase genes, and transposase genes, in addition to mutations in genes related to putative proteins and proteins of unknown function. These mutated genes may be associated with gene expression, metabolism and signaling, and DNA methylation. By regulating the expression of the key genes in the microbial metabolic pathway, it can promote metabolism, accelerate the influx of nutrients and produce the efflux of inhibitors, leading to increase of ethanol production (Nataf *et al*. 2010).

There were 70 structural variants in C0, including 7 intrachromosomal migrations, 60 deleted SVs, and 3 inverted SVs. There were 66 structural variants in C1, including 6 intrachromosomal migrations, 57 deleted SVs, and 3 inverted SVs. There were 80% of SVs with length of 1000 bp or more. The SVs in this experiment mainly involved integrase catalytic region, transposase, and transcription terminator Rho. The outermost circle in Fig. 7 shows the coordinates of the reference sequence positions, and from the outer to the inner, the InDel distribution, SNP number distribution, reads coverage depth, reference sequence genomic GC content, and reference sequence genomic GC offset value distribution of C0 and C1, respectively. The data indicated that neodymium (Nd) ions induced multiple mutations in the genome of *C. thermocellum* ATCC C0, with the single nucleotide polymorphism (SNP) and structural variation (SV) data supporting one another.

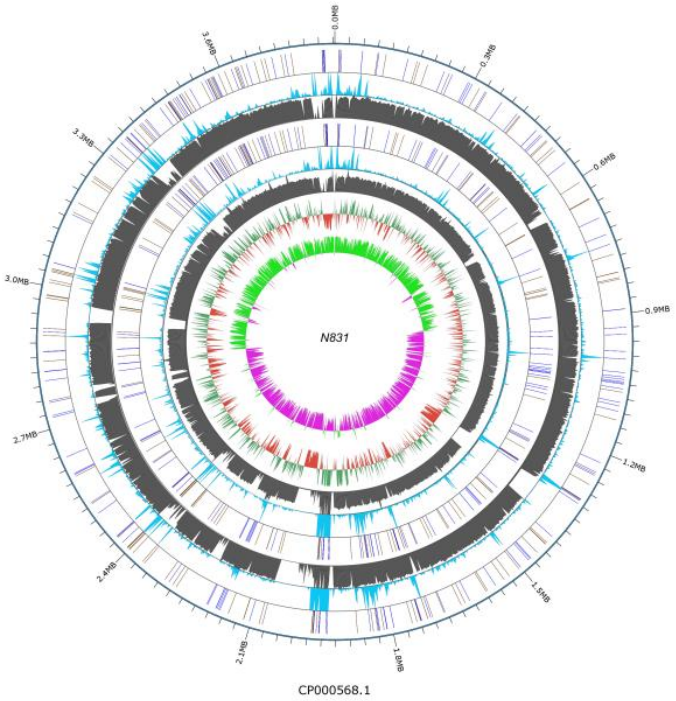

Fig. 7. Genome-wide variation map

Results of Knockout Strains Growth Measurement

The strain of *C. thermocellum* C0 with arac knocked out will be abbreviated as CX, the strain with *mcp* knocked out as CY, and the strain with *Type* gene knocked out as CG. The knockout strains were identified and successfully constructed. As shown in Fig. 8, the three deletion strains of CX, CY, and CG and the wild strain all showed a typical "S" shaped growth curve, and the time of the delayed, logarithmic growth period and stable period of both were basically the same. The experimental results indicated that the knockdown of the three genes respectively did not produce significant effects on bacterial growth and reproduction. This observation may be attributed to the fact that the gene knockdown did not affect the biomass of *C. thermocellum*, resulting in similar growth trends among the strains (Lo *et al*. 2010).

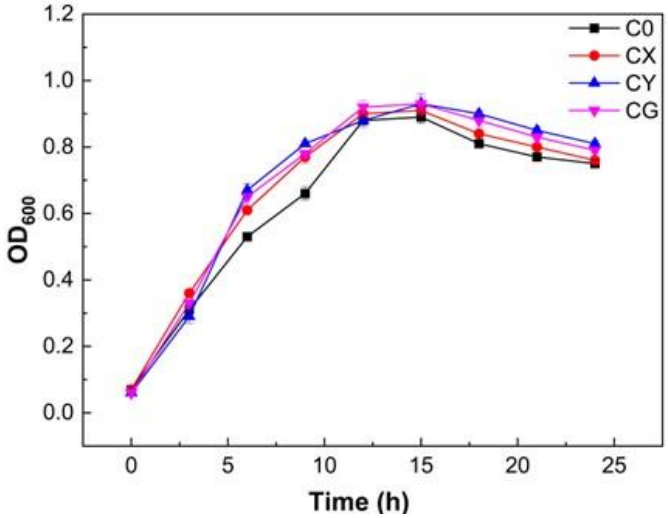

Fig. 8. Growth curve of original strain and knockout strains

Results of Ethanol Yield Measurement of Knockout Strains

As shown in Fig. 9, there was no significant change in ethanol production of CX strain after knocking down arac compared to the original strain.

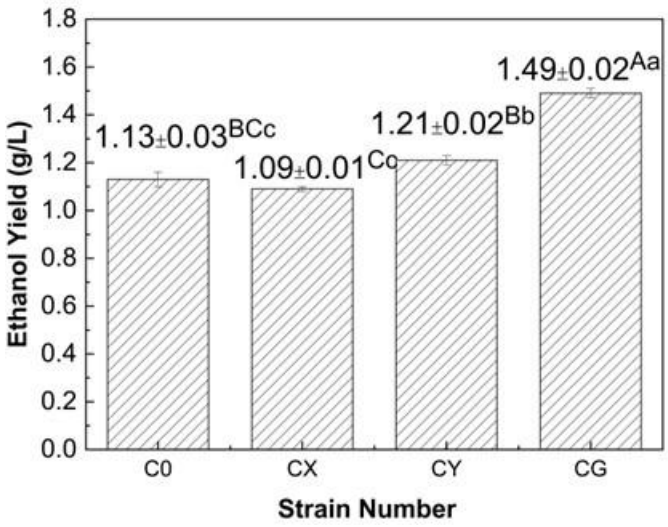

Fig. 9. Ethanol production of original strains and knockout strains; Different lowercase letters mean that $p < 0.05$, and different uppercase letters mean that $p < 0.01$

The ethanol production of CY strain with *MCP* knockdown was 1.07 times higher than that of the original strain. The ethanol yield of CG strain with knockout of *Type* was 1.32 times higher than that of the original strain. This indicates that the *Arac* gene is not a key locus for Nd^{3+} to improve ethanol yield, while the mutations in *MCP* and Type are associated with ethanol yield improvement to some extent. Fu *et al*. (2019) increased the ethanol yield of *Thermoanaerobacterium aotearoense* SCUT27 with 15.8% by gene knockout. The ethanol yield of CG in this experiment was increased with 31.9%, which was higher than the cited study.

Mutations in the AraC gene did not significantly impact ethanol production. However, these mutations may influence the expression of genes related to cell membrane formation in *C. thermocellum* C0, potentially enhancing the uptake nutrients or the excretion of product inhibitors (Wang *et al*. 2022; Santiago *et al*. 2016). It is plausible that this gene plays a role in the regulation of gene expression within other metabolic pathways, potentially influencing the improvement of ethanol production. The primary function of this gene type is to bind to the substrate cellulose. Variations in the cellulose degradation capacity of cellulosomes can be attributed to differences in structural components and assembly patterns across various microbial species. (Sheng *et al*. 2022).

CONCLUSIONS

1. The analysis conducted through sequencing revealed the presence of mutations in the promoter regions of the genes alcohol dehydrogenase (ADH), pyruvate-ferric redox protease (PFO), and 6-phosphofructokinase (PFK).
2. The findings from results of the targeted mutation assay suggest that the alteration in PFO enzyme expression is attributable to a mutation within the promoter sequence.
3. The sequencing results revealed the presence of 93 mutations in C1, encompassing genes associated with cell membrane biosynthesis, methyl chemotaxis receptor proteins, ribonucleases, endonucleases, transcriptional regulators, methyltransferases, and transposases.
4. The knockout of the key genes arac, mcp, and type 3a cellulose-binding domain protein (Type) did not impact the growth of the strain, however, mutations in the methyl-accepting chemotaxis proteins (MCP) and Type genes were correlated with enhanced ethanol production.

ACKNOWLEDGMENTS

The authors are grateful for the support of the Inner Mongolia Scientific Research Fund for Outstanding Youth Scholar (2022JQ10) and the National Natural Science Foundation of China (32060017).

REFERENCES CITED

Bayer, E. A., Belaich, J. P., Shoham, Y., and Lamed, R. (2004). "The cellulosomes: Multienzyme machines for degradation of plant cell wall polysaccharides," *Annual Review of Microbiology* 58, 521-554. DOI: 10.1146/annurev.micro.57.030502.091022

Biswas, R., Zheng, T., Olson, D. G., Lynd, L. R., and Guss, A. M. (2015). "Elimination of hydrogenase active site assembly blocks H_2 production and increases ethanol yield in *Clostridium thermocellum*," *Biotechnology for Biofuels* 8, article 20. DOI: 10.1186/s13068-015-0204-4

Brown, S. D., Guss, A. M., Karpinets, T. V., Parks, J. M., Smolin, N., Yang, S., Land, M. L., Klingeman, D. M., Bhandiwad, A., Rodriguez, Jr., M., *et al.* (2011). "Mutant alcohol dehydrogenase leads to improved ethanol tolerance in *Clostridium thermocellum*," *Proceedings of the National Academy of Sciences of the United States of America* 108(33), 13752-13757. DOI: 10.1073/pnas.1102444108

Carere, C. O., Rydzak, T., Cicek, N., Levin, D. B., and Sparling, R., (2014). "Role of transcription and enzyme activities in redistribution of carbon and electron flux in response to N_2 and H_2 sparging of open-batch cultures of *Clostridium thermocellum* ATCC 27405," *Applied Microbiology & Biotechnology* 98(6), 2829-2840. DOI: 10.1007/s00253-013-5500-y

Chang, Y.-C., Lee, W.-J., Lin, S.-L., and Wang, L.-C. (2013). "Green energy: Water-containing acetone–butanol–ethanol diesel blends fueled in diesel engines," *Applied Energy* 109, 182-191. DOI: 10.1016/j.apenergy.2013.03.086

Darnall, D. W., and Birnbaum, E. R. (1970). "Rare earth metal ions as probes of calcium ion binding sites in proteins," *Journal of Biological Chemistry* 245(23), 6484-6486. DOI:10.1016/B978-0-444-53159-9.00012-7

Desai, S. G., Guerinot, M. L., and Lynd, L. R. (2004). "Cloning of l -lactate dehydrogenase and elimination of lactic acid production via gene knockout in *Thermoanaerobacterium saccharolyticum* JW/SL-YS485," *Applied Microbiology & Biotechnology* 65(5), 600-605. DOI10.1007/s00253-004-1575-9

Diatloff, E., Smith, F. W., and Asher, C. J. (1995). "Rare earth elements and plant growth: I. Effects of lanthanum and cerium on root elongation of corn and mungbean," *Journal of Plant Nutrition* 18, 1963-1976. DOI: 10.1080/01904169509365037

Fu, H., Yang, X., Qu, C., and Wang, J. F. (2019). "Enhanced ethanol production from lignocellulosic hydrolysates by inhibiting the hydrogen synthesis in *Thermoanaerobacterium aotearoense* SCUT27(*ΔIdh*)," *Journal of Chemical Technology & Biotechnology* 94, 3305-3314. DOI:10.1002/jctb.6141

Furukawa, T., Shida Y., Kitagami N., Mori K., Kato M., Kobayashi T., Okada H., Ogasawara W., and Morikawa Y. (2009). "Identification of specific binding sites for XYR1, a transcriptional activator of cellulolytic and xylanolytic genes in *Trichoderma reesei*," *Fungal Genetics & Biology* 46(8), 564-574. DOI: 10.1016/j.fgb.2009.04.001.

Gomez, J. E., Birnbaum, E. R., and Darnall, D. W. (1974). "The metal ion acceleration of the conversion of trypsinogen to trypsin. Lanthanide ions as calcium ion substitutes," *Biochemistry* 13(18), 3745-3750. DOI:10.1021/bi00715a020

Guo, Y., Liu, G., Ning, Y., Li, X., Hu, S., Zhao, J., and Qu, Y. (2022). "Production of cellulosic ethanol and value-added products from corn fiber," *Bioresources and Bioprocessing* 9, article 81. DOI: 10.1186/s40643-022-00573-9

Hosseini, S. E., and Wahid, M. A. (2013). "Feasibility study of biogas production and utilization as a source of renewable energy in Malaysia," *Renewable and Sustainable Energy Reviews* 19(5), 454-462. DOI: 10.1016/j.rser.2012.11.008

Huang, X., Li, Z., Du, C., Wang, J., and Li, S. (2015). "Improved expression and characterization of a multidomain xylanase from *Thermoanaerobacterium aotearoense* SCUT27 in *Bacillus subtilis*," *Journal of Agricultural and Food Chemistry* 63(28), 6430-6439. DOI: 10.1021/acs. jafc.5b01259

Jayakumar, M., Gebeyehu, K. B., Abo, L. D., Tadesse, A. W., Vivekanandan, B., Sundramurthy, V. P., Bacha, W., Ashokkumar, V., and Baskar, G. (2023). "A comprehensive outlook on topical processing methods for biofuel production and its thermal applications: Current advances, sustainability and challenges," *Fuel* 349, article ID 128690. DOI: 10.1016/j.fuel.2023.128690

Jiang, Y. Z., Yuan, X. Y., Huang, H. B., Wang, D., Liu, R. M., Wang, H. L., and Teng, F. (2021). "Research progress and the biotechnological applications of multienzyme complex," *Applied Microbiology and Biotechnology* 105(5), 1759-1777. DOI: 10.1007/s00253-021-11121-4

Joan, G., Marcano-Velazquez, J., Lo, A., Maness, P.-C., and Chou, K. J. (2019). "Developing riboswitch-mediated gene regulatory controls in thermophilic bacteria," *ACS Synthetic Biology* 8(4), 633-640. DOI: 10.1021/acssynbio.8b00487

Kannuchamy, S., Mukund, N., and Saleena, L. M. (2016). "Genetic engineering of *Clostridium thermocellum* DSM1313 for enhanced ethanol production," *BMC Biotechnology* 16(1), article 34. DOI: 10.1186/s12896-016-0260-2

Leacock, S. W., and Reinke, V. (2006). "Expression profiling of MAP kinase–mediated meiotic progression in *Caenorhabditis elegans*," *Plos Genetics* 2(11), article e174. DOI: 10.1371/journal.pgen.0020174

Levin, D. B., Islam, R., Cicek, N., and Sparling, R. (2006). "Hydrogen production by *Clostridium thermocellum* 27405 from cellulosic biomass substrates," *International Journal of Hydrogen Energy* 31(11), 1496-1503. DOI: 10.1016/j.ijhydene.2006.06.015

Liu, Y. J., Li, B., Feng, Y. G., and Cui, Q. (2020). "Consolidated bio-saccharification: Leading lignocellulose bioconversion into the real world," *Biotechnology Advances* 40, article ID 107535. DOI: 10.1016/j.biotechadv.2020.107535

Liyakathali, N. A. M., Muley, P. D., Aita, G., and Boldor, D. (2016). "Effect of frequency and reaction time in focused ultrasonic pretreatment of energy cane bagasse for bioethanol production," *Bioresource Technology* 200, 262-271. DOI: 10.1016/j.biortech.2015.10.028

Lo, J., Zheng, T., Hon, S., Olson, D. G., Lynd, L. R., and Metcalf, W. W. (2015). "The bifunctional alcohol and aldehyde dehydrogenase gene, *adh*E, is necessary for ethanol production in *Clostridium thermocellum* and *Thermoanaerobacterium saccharolyticum*," *Journal of Bacteriology* 197(8), 1386-1393. DOI: 10.1128/JB.02450-14

Lovett, J. C., Hards, S., Clancy, J., and Snell, C. (2011). "Multiple objectives in biofuels sustainability policy," *Energy & Environmental Science* 4, 261-268. DOI: 10.1039/c0ee00041h

Mazzoli, R., and Olson, D. G. (2020). "*Clostridium thermocellum*: A microbial platform for high- value chemical production from lignocellulose," *Advances in Applied Microbiology* 07, 111-161. DOI: 10.1016/bs.aambs.2020.07.004

Mikel, I. O., and Orna, A. C. (2021). "Coupled transcription-translation in prokaryotes: An old couple with new surprises," *Frontiers in Microbiology* 11. DOI: 10.3389/fmicb.2020.624830.

Myat, L., and Ryu, G.-H. "Thermomechanical extrusion and sodium hydroxide pretreatments for ethanol production from destarched corn fiber," *Environmental Progress & Sustainable Energy* 34, article ID 12059. DOI: 10.1002/ep.12059

Nataf, Y., Bahari, L., Kahel-Raifer, H., Borovok, I., Lamed, R., Bayer, E. A., Sonenshein, A. L., and Shoham, Y. (2010). "*Clostridium thermocellum* cellulosomal genes are regulated by extracytoplasmic polysaccharides *via* alternative sigma factors," *Proceedings of the National Academy of Science* 107(43), 18646-18651. DOI: 10.1073/pnas.1012175107

Nawab, S., Zhang, Y. F., Ullah, M. W., Lodhi, A. F., Shah, S. B., Rahman, M. U., and Yong, Y. C. (2024). "Microbial host engineering for sustainable isobutanol production from renewable resources," *Applied Microbiology and Biotechnology* 108, 16-18. DOI: 10.1007/ s00253-023-12821-9

Nur Aimi, M. N., Anuar, H., Nurhafizah, S. M., and Zakaria, S. (2015). "Effects of dilute acid pretreatment on chemical and physical properties of kenaf biomass," *Journal of Natural Fibers* 12(3), 256-264. DOI: 10.1080/15440478.2014.919894

Pang, J., Hao, M., Li, Y. L., Liu, J. G., Lan, H., Zhang, Y. F., and Liu, Z. Y. (2018a). "Consolidated bioprocessing using *Clostridium thermocellum* and *Thermoanaerobacterium thermosaccharolyticum* co-culture for enhancing ethanol production from corn straw," *BioResources* 13(4), 8209-8221. DOI: 10.15376/biores.13.4.8209-8221

Pang, J., Hao, M., Shi, Y. L., Li, Y. L., Zhu, M. D., Hu, J. H., Zhang, Q. C., and Liu, Z. Y. (2018b). "Enhancing the ethanol yield from salix using a *Clostridium thermocellum* and *Thermoanaerobacterium thermosaccharolyticum* co-culture system," *BioResources* 13(3), 5377-5393. DOI: 10. 15376/BIORES.13.3.5377-5393

Petsch, B., Schnee, M., Vogel, A. B., Lange, E., Hoffmann, B., Voss, D., Schlake, T., Thess, A., Kallen, K. J., Stitz, L., *et al*. (2012). "Protective efficacy of *in vitro* synthesized, specific mRNA vaccines against influenza A virus infection," *Nature Biotechnology* 30(12), 1210-1216. DOI: 10.1038/nbt.2436

Qiao, J., Cui, H. Y., Wang, M. H., Fu, X. S., Wang, X. Y., Li, X. J., and Huang, H. (2022). "Integrated biorefinery approaches for the industrialization of cellulosic ethanol fuel," *Bioresource Technology* 360, article ID 127516. DOI: 10.1016/j.biortech.2022.127516

Reijnders, L., and Huijbregts, M. A. J. (2007). "Life cycle greenhouse gas emissions, fossil fuel demand and solar energy conversion efficiency in European bioethanol production for automotive purposes," *Journal of Cleaner Production* 15(18), 1806-1812. DOI: 10.1016/j.jclepro.2006.05.007

Santiago, A. E., Yan, M. B., Tran, M., Wright, N., Luzader, D. H, Kendall, M. M., Ruiz-Perez, F., and Nataro, J. P. (2016). "A large family of anti-activators accompanying XylS/AraC family regulatory proteins," *Molecular Microbiology* 101(2), 314-332. DOI: 10.1111/mmi.13392

Shaw, A. J., Jenney, F. E., Adams, M. W. W., and Lynd, L. R. (2008). "End-product pathways in the xylose fermenting bacterium, *Thermoanaerobacterium*

saccharolyticum," *Enzyme and Microbial Technology* 42(6), 453-458. DOI: 10.1016/j.enzmictec.2008.01.005

Sheng, T., Meng, Q. B., Li, Z. L., Sun, C. Y., Li, L. X., and Liu, L. L. (2022). "Comparative genomics reveals cellobiose hydrolysis mechanism of *Ruminiclostridium thermocellum* M3, a cellulosic saccharification bacterium," *Frontiers in Microbiology* 13, article ID 1079279. DOI: 10.3389/fmi cb.2022.1079279

Sindhu R., Kuttiraja M., Binod P., Sukumaran R. K., and Pandey A. (2014). "Physicochemical characterization of alkali pretreated sugarcane tops and optimization of enzymatic saccharification using response surface methodology," *Renewable Energy* 62, 362-368. DOI: 10.1016/j.renene.2013.07.041

Singh, S., Kumar, A., Sivakumar, N., and Verma, J. P. (2022). "Deconstruction of lignocellulosic biomass for bioethanol production: Recent advances and future prospects," *Fuel* 327, article ID 125109. DOI: 10.1016 /j.fuel.2022.125109

Sridhar, J., Eiteman, M. A., and Wiegel, J. W. (2000). "Elucidation of enzymes in fermentation pathways used by *Clostridium thermosuccino* genes growing on inulin," *Applied and Environmental Microbiology* 66(1), 246-251. DOI: 10.1128/AEM.66.1.246-251.2000

Wang, Y. B., Hu, J. H., Li, Y. L., and Liu, Z. Y. (2022). "Rare earth ion Nd^{3+} promotes production of cellulose ethanol by *Clostridium thermocellum* ATCC 27405," *Polyhedron* 211, article ID 115555. DOI: 10.1016/j.poly.2021.115555

Würleitner, E., Pera, L., Wacenovsky, C., Cziferszky, A., Zeilinger, S., Kubicek, C. P., and Mach, R. L. (2003). "Transcriptional regulation of *xyn2* in *Hypocrea jecorina*," *Eukaryotic Cell* 2, 150-158. DOI: 10.1128/EC.2.1.150-158.2003

Xiao, Y., Dong, S., Liu, Y. J., You, C., Feng, Y. G., and Cui, Q. (2023). "Key roles of β-glucosidase BglA for the catabolism of both laminaribiose and cellobiose in the lignocellulolytic bacterium *Clostridium thermocellum*," *International Journal of Biological* 250, article ID 126226. DOI: 10.1016/ j.ijbiomac.2023.126226

Xin, W. K., and Gao, X. X. (1996). "Study of the effect of lanthanide ions on the kinetics of glutamate dehydrogenase by a chronoamperometric method," *Analyst* 121(5), 687-690. DOI: 10.1039/A N9962100687

Yayo, J., Kuil, T., Olson, D. G., Lynd, L. R., and Maris, A. J. A. V. (2021). "Laboratory evolution and reverse engineering of *Clostridium thermocellum* for growth on glucose and fructose," *Applied and Environmental Microbiology* 87(9), article ID e03017-20. DOI: 10.1128/AEM.03017-20

Yu, M., Li, J., Li, S., Du, R., Jiang, Y., Fan, G., and Chang S. (2014). "A cost-effective integrated process to convert solid-state fermented sweet sorghum bagasse into cellulosic ethanol," *Applied Energy* 115(15), 331-336. DOI: 10.1016/j.apenergy.2013.11.020

Zeng, M., Mosier, N. S., Huang, C. P., Sherman, D. M., and Ladisch, M. R. (2010). "Microscopic examination of changes of plant cell structure in corn stover due to hot water pretreatment and enzymatic hydrolysis," *Biotechnology & Bioengineering* 97(2), 265-278. DOI:10.1002/bit.21298

Zhang, D. Y., Hu, J. H., Bater Siqin, Zhang, T., and Chang, Y. (2009). "Dy^{3+} and Nd^{3+} induced genetic mutation of bacillus α-amylase," J*ournal of Inorganic Biochemistry* 103(7), 935-939. DOI: 10.1016/j.jinorgbio.2008.12.002

Zhang, J., Liu, S., Li, R., Hong, W., Xiao, Y., Feng, Y., Cui, Q., and Liu, Y. J. (2017). "Efficient whole- cell-catalyzing cellulose saccharification using engineered

Clostridium thermocellum," *Biotechnology for Biofuels* 10, 124-138. DOI: 10.1186/s13068-017-0796-y

Zheng, X., Xian, X., Hu, L., Tao, S., Zhang, X., Liu, Y., and Lin, X. (2021). "Efficient short-time hydrothermal depolymerization of sugarcane bagasse in one-pot for cellulosic ethanol production without solid-liquid separation, water washing, and detoxification," *Bioresource Technology* 339, article ID 125575. DOI: 10.1016/j.biortech.2021.125575

Article submitted: August 08, 2024; Peer review completed: November 15, 2024; Revised version received: January 5, 2025; Accepted: February 23, 2025; Published: March 7, 2025.
DOI: 10.15376/biores.20.2.3155-3175